Application and Optimization of Mesh Simplification in 3D virtual Reality Scene in a High-performance Environment

Jing He[1*], Peizhuo Wang[2], Jiayi Zhu[1] and Jichao Zeng[3]

{*Corresponding author: bhhejing@buaa.edu.cn}

{wangpeizhuo_37@163.com, sunyu878484303@163.com, 550654676@qq.com}

[1]Institute for Advanced Studies in Humanities and Social Science, Beihang University, Beijing 100183, China

[2]Institute for Interdisciplinary Information Sciences, Tsinghua University, Beijing 100084, China

[3] GuangHan College, Civil Aviation Flight University of China, SiChuan, 618311, China

Abstract. Real-time 3D imaging and display technology in virtual reality technology has become a key research object; However, modern computer work has been dramatically improved compared with the past; it still cannot meet the requirements of drawing real-time complex scenes and objects. Level of detail modeling technology is the most promising technology for 3D images, which is to develop a set of models with different levels of polygonal information from the same original model describing an event or object. Based on the above background, this article puts forward the application of 3D modeling-based LOD technology in virtual reality as the research goal, studies the concept of LOD technology in detail, analyzes the QEM algorithm, and then researches and optimizes the QEM algorithm. According to the experimental research in this article, the basic algorithm used in simplifying the initial model can simplify the model to a certain extent, but the data could be better. Using an immune genetic algorithm to facilitate nodes has succeeded dramatically, saving nearly 50% of nodes and about 90% of the time based on the most straightforward optimization. However, in this case, the model cannot display details.

Keywords: 3D Modeling, Virtual Reality Technology, Lod Technology, Immune Genetic Algorithm

1 Introduction

In recent years, with the development of computing power and the rapid growth of graphics, 3D imaging technology has also been widely used as the first research content of pictures [1]. 3D visualization refers to using graphics technology, imaging technology, and virtual reality technology in specific 3D graphics to draw clear three-dimensional graphics based on abstract data on the screen, allowing people to understand more intuitively [2].

The technical stage of the level of detail model should start from a geometric point of view to reduce the complexity of the geometrical surface of the model, thereby reducing the number of triangles that represent objects or events [3]. The main content of the model level description

ICSETPSD 2023, November 17-18, Coimbatore, India

DOI 10.4108/eai.17-11-2023.2342816

includes 1) Simplification of the model is to study what methods should be used to reduce the number of triangles on the model. 2) The error when the model is flexible is a method to ensure the similarity between the simple model and the original model, and the level of detail of these models has changed the traditional view that the more triangles, the higher the quality of the model. According to the complexity of the image settings and events, an appropriate detail model is created and selected for the object, ensuring that the scene or model is drawn in real time while meeting the visual effect requirements [4].

As for the research on the generation algorithm of the LOD model, by analyzing and comparing the simplified signal of the model with the existing simplified model algorithm, it is found that the curvature is helpful to the quantification of the triangular mesh in the calculation of the curve and the edge folding algorithm [5]. Discussing the edge folding algorithm and the introduction of curvature in the LOD technology to improve the secondary error measurement to ensure that the simple model and the original model have a certain degree of similarity, achieve the best results, and improve the algorithm of the progressive network, making it possible to display the level of detail of the model quickly [6].

2 Application of VR technology and Lod technology

2.1 Detailed Selection of the Model

The simplification technology of the LOD model is used to create different levels of mirror images of the same model because selecting the appropriate model when drawing the model can improve efficiency. The selection methods of the model mainly include:

(1) Distance selection method: In the process of model components, the distance selection method selects the model according to the distance between predefined points on the object, and this method is the simplest and the most effective. When the thing is too far away from the viewpoint, the model's details are unimportant and occupy fewer pixels on the screen; we can choose a rough model. When the object is close to the viewpoint, it is necessary to pay attention to the details of the model and select the appropriate model to construct the component [7].

(2) Size selection method: In model building, select the model according to the size of the screen that the model occupies.

(3) Eccentricity selection method: In model building, select the required model according to the degree of deviation of the model from the center of the screen. Generally speaking, users are most concerned about the screen's center point. When the model is too far from the center, the visual information generated by the user will be reduced, so the fineness of the model will be reduced accordingly.

(4) Speed property method: In model building, select the appropriate detail model according to the model's speed relative to the viewpoint. When the model moves faster in the scene, the less visual information the eyes receive, so the key of this method is to establish a set of metric standards between the movement speed of the model and the degree of detail of the model [8].

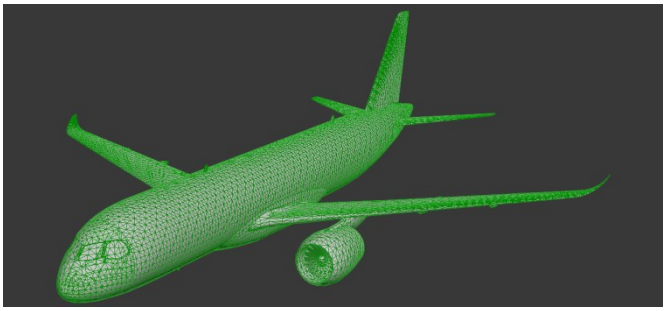

Fig.1 Schematic diagram of the mesh triangle model based on the LOD algorithm

2.2 Simplified Algorithm of Lod Model

(1) Secondary error measurement

As shown in Figure 1, the quadratic error metric is used as the calculation standard of the folding cost. Assuming that each edge in the original grid has a corresponding error matrix Q, assuming that the folding point of T_i is $V_{10} = [x_{10}, y_{10}, z_{10}]^T$, then the folding cost of this point can be calculated according to the following formula:

$$\begin{aligned}\varepsilon(T_i) &= V_{i0}^T Q_i V_{i0} \\ &= q_{i11}x_{i0}^2 + 2q_{i12}x_{i0}y_{i0} + 2q_{i13}x_{i0}z_{i0} + 2q_{i14}x_{i0} + q_{i22}y_{i0}^2 \\ &+ 2q_{i23}x_{i0}z_{i0} + 2q_{i24}y_{i0} + q_{i33}z_{i0}^2 + 2q_{i34}z_{i0} + q_{i44}\end{aligned} \tag{1}$$

There are various positions in this formula. Theoretically, we can replace v_{i0}, which $\varepsilon(T_i)$ is the minimum value. When the partial derivative of the above procedure is taken and set to 0, then the process is:

$$\begin{bmatrix} q_{i11} & q_{i12} & q_{i13} & q_{i14} \\ q_{i12} & q_{i22} & q_{i23} & q_{i24} \\ q_{i13} & q_{i23} & q_{i33} & q_{i34} \\ 0 & 0 & 0 & 1 \end{bmatrix} = v_{i0} \begin{bmatrix} 0 \\ 0 \\ 0 \\ 1 \end{bmatrix} \tag{2}$$

Assuming that this system of equations can be solved, it can be obtained according to formula (5), namely:

$$v_{i0} = \begin{bmatrix} q_{i11} & q_{i12} & q_{i13} & q_{i14} \\ q_{i12} & q_{i22} & q_{i23} & q_{i24} \\ q_{i13} & q_{i23} & q_{i33} & q_{i34} \\ 0 & 0 & 0 & 1 \end{bmatrix}^{-1} \begin{bmatrix} 0 \\ 0 \\ 0 \\ 1 \end{bmatrix} \tag{3}$$

This method is calculated based on the positions of a midpoint and two vertices of this edge so that the minor position of these three points is the position of v_{i0} according to formula (6) [9].

For each edge in the grid, we can find the triangle set C_i related to the two vertices associated with this edge, and the error is the point $\varepsilon(T_i)$ obtained by calculating this point. The specific formula is:

$$\varepsilon(T_i) = \sum_i (p_i^T v_{i0})^2 \tag{4}$$

It represents the plane equation T_i of the plane where the triangle related to the triangle $ax + by + cz + d = 0$ $a^2 + b^2 + c^2 = 1$ is located, and the obtained formula is:

$$\varepsilon(T_i) = \sum_{p \in c} ((v_{i0}^T p)(p^T v_{i0})) = \sum_{p \in c} (v_{i0}^T (pp^T) v_{i0}) = v_{i0}^T \sum_{p \in c} (M_p) v_{i0} \tag{5}$$

The M_p in this formula is a symmetric matrix if it becomes a triangular error matrix, as shown below:

$$M_p = pp^T = \begin{bmatrix} aa & ab & ac & ad \\ ab & bb & bc & bd \\ ac & bc & cc & cd \\ ad & bd & cd & dd \end{bmatrix} \tag{6}$$

Solve the triangular error matrix related to the point; the error matrix Q_i about the point v_{i0} can be obtained [10].

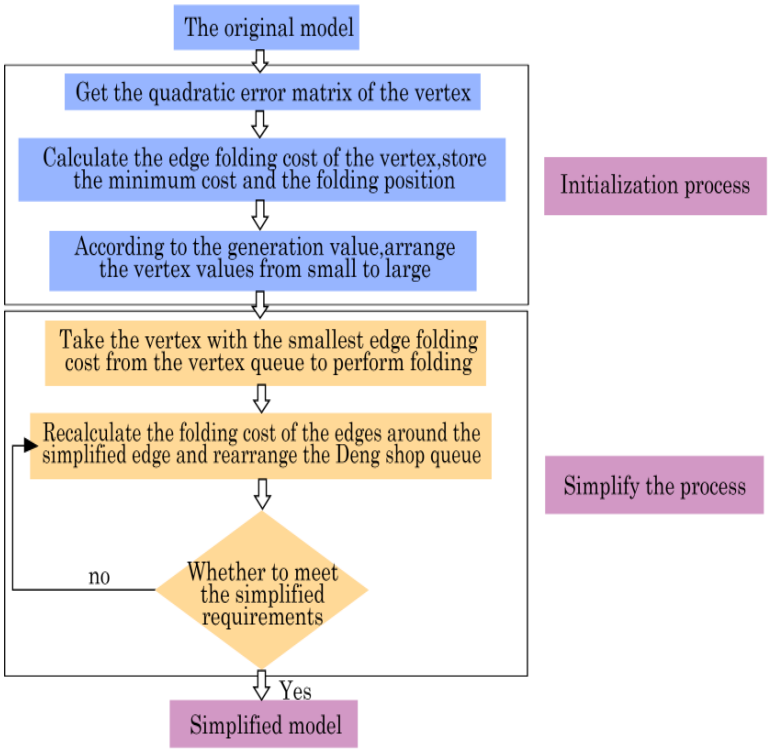

Fig.2 Flow chart of edge folding algorithm based on QEM algorithm

As shown in Figure 2, the best-simplified algorithm can maintain the geometric features of the model, such as the topological system, sharp edges, and edges of the model, while minimizing the vertical and triangular edges of the mesh.

(2) Improve QEM algorithm

Because the value of the secondary error measurement includes the measurement distance, the simple mesh distribution is uniform. After large-scale adjustment, the simple model will lose important geometric features such as sharp edges and angles in the original model. Therefore, when the model is flexible, using the product of the squared error table and the perfect vertex alignment as the new error table [11], the reasons are as follows:

In the mesh simplification algorithm, multiplying the adaptive value and the error matrix K_p will not change the secondary error matrix's properties. However, compared with absolute and Gaussian mean curvature, only the model edge folding reading order has more advantages. Due to its unique properties, total curvature is suitable for simplifying the triangular mesh model. The average curvature represents the curvature of many adjacent triangular faces. Assuming that V is the endpoint and e_i is the side, the formula for the average curvature is:

$$H = (\sum m(e_i)) / A \tag{7}$$

In the formula, A is the vertex V is the sum of the areas of the related triangles, and $m(e_i)$ represents the angle between the normal vectors of the triangles adjacent to e_i, as shown in Figure 5. The normal vectors of triangles T_1 and T_2 adjacent to e_i are n_1 and n_2, respectively, and the angle between the two is φ, that is, $m(e_i)$, and the formula is expressed as:

$$\cos\varphi = \cos < n_1, n_2 >= \frac{n_1 n_2}{| n_1 || n_2 |} \tag{8}$$

Gaussian curvature represents the curvature of a curved surface, an essential geometric quantity in a curved surface, and the meaning of the absolute value K is undeniable. Assuming that the value of the small cover on the large shell is $\Delta\partial$, then the area of this trim surface is $\Delta\partial$, And it includes point P, and translate the vector of $\Delta\partial$ toward n to the origin of E3, the scoring area $\Delta\partial^*$ of the surface S2 with the head as the center can be obtained. Then the curve degree of the surface in P is the ratio of $\Delta\partial$ to $\Delta\partial^*$, and the formula used is:

$$K = (2\pi - \sum_{i=1}^{k} \theta_i) / A \tag{9}$$

The θ_i D in the formula represents the angle related to v. The two permission bending rates for setting v are k_1, k_2, The curvature of the two curves is:

$$\begin{aligned} k_1 &= H + \sqrt{H^2 - K} \\ k_2 &= H - \sqrt{H^2 - K} \end{aligned} \tag{10}$$

If $H^2 - k < 0$, then make $H^2 - k = 0$, the absolute curvature K_{abs} of vertex v can be obtained as:

$$K_{abs} = | k_1 | + | k_2 | \tag{11}$$

Assuming that edge (v_i, v_j) is folded to a new vertex $\bar{v}$, the optimized cost formula is:

$$\Delta''(\bar{v}) = \| v_i v_j \| \bar{V}^T (K_{iabs} Q_i^{'} + K_{jabs} Q_j^{'}) \bar{v} \tag{12}$$

The formula $\| v_i v_j \|$ represents the distance between the v_i, v_j vertices K_{iabs}, K_{jabs}, is the total curve rate of the two vertices, and Q'_i, Q'_j is the error matrix of the two vertices.

(3) Immune genetic algorithm

The immune genetic algorithm is developed based on the natural immune system's adaptive identification and elimination of antigens and foreign bodies that invade the body. It forms a set of unique solving algorithms through abstract mathematical Modeling of the biological immune system's learning, memory, and adaptive adjustment capabilities and is integrated into the genetic algorithm. The steps and formulas of the immune genetic algorithm are as follows:

$$\begin{cases} \min f(x(1), x(2), ...x(p)) \\ a(j) \le x(j) \le b(j), j = 1,2,3,....p \end{cases} \quad (13)$$

In the above formula, $x(j)$ the optimization variable $[a(j), b(j)]$ is the interval range of the value $x(j)$, and P is the number of generation optimization.

1) Resistant original actual number coding

Immune genetic algorithm uses binary coding, which has the advantage of solid search ability but requires much calculation (coding and conversion) and cannot generate enough values. In contrast, real-time coding can significantly reduce the statistical significance. According to the vaccine genetic algorithm, the antibody code is obtained, and each antibody corresponds to a solution to the problem, so the coding region and the antibody solution have a one-to-one correspondence, and it can be coded as follows:

$$x(j) = a(j) + u_0(j) * (b(j) - a(j)), (j = 1, ...n) \quad (14)$$

After compilation, the j optimized variable $x(j)$ with the initial value range $[a(j), b(j)]$ Can be reflected on real numbers $y(j)$. The interval of the actual number is between [0,1], assuming that $y(j)$ it will be a gene, then the calculation form is:

$$(y(1), y(2), ...y(p)) \quad (15)$$

2) Production of initial antibody

Under certain conditions, set to produce n groups of random numbers on the interval [0,1], each group has m. Selected $u_0(j,i)$ as the parent value $y(j,i)$ of the initial population and substitute into the formula to obtain the optimized variable value $x(j,i)$ and the corresponding objective function value $f(i)$.

3) Extract the vaccine

From the previous step to excellent individuals, perform gene extraction, evaluate the affinity

of each gene, select the best set of genes, and find the average number of gene $y(j)$ s as the vaccine K.

4) Affinity calculation

Substitute $x_j(i)$ into $\min |f(x)|, x \in D$, f is the objective function, X is the excellent individual, and D is the domain solution. The larger the included value $f(i)$, Then the affinity of the individual is smaller. Finally, define the affinity function value as:

$$F(i) = \begin{cases} 1/f^2(i), f(i) \neq 0 \\ M_{\max}, f(i) = 0(1.....m) \end{cases} \tag{16}$$

Because $M_{\max}$ it represents a large enough positive number N_0 in the preliminary search algebra.

5) Judgment of the immune algorithm

We need to select N excellent individuals as the parent, establish P_i and $P_i > 0, P_1 + P_2 + ...P_n = 1$ that is inversely proportional to the affinity function value f_i, and select 2M unique individual groups to form a new population $U_c(j,i)$.

6) Single crossover and algorithm mutation

Combine the individual parts of the two parents according to the crossover probability P_c according to a specific mechanism, and then suppose that the clone is paired with M pairs of individuals. Any team of individuals needs to meet the following:

$$U_c(j,i) = \begin{cases} u_{x1} * u_{oc}(j,i_1) + (1-u_{x1}) u_{oc}(j,j_2), u_x < 0.5 \\ u_{x2} * u_{oc}(j,j_1) + (1-u_{x1}) u_{oc}(j,j_2), u_x \geq 0.5 \end{cases} \tag{17}$$

In the new group $U_c(j,i)$, using P_m the mutation. If it is too small, it will cause the algorithm to converge locally, and if it is too large, it will destroy the group model, and the generated variant individuals are $U_p(j,i)$ operations:

$$U_p(j,i) = \begin{cases} u_c(j,i), u_x \geq p_m \\ u(j), u_x < p_m \end{cases} \tag{18}$$

3 Algorithm Experiment Results

The experimental environment in this experiment is Windows 10, a 64-bit operating system; the CPU is an Intel Core i5-10400 processor with 16GB of memory, and The graphics card is a

1660 graphics card with 6G of memory. In this experiment, different models were selected for simplification, and various algorithms were used for comparison and analysis based on the simplified model's geometric error, visual quality, and grid distribution.

3.1 Garland Algorithm Optimizes Qem Algorithm

As shown in Table 1, a model with cattle as the prototype was selected for error comparison, and many experiments were carried out according to different numbers of faces.

Table 1. Error Comparison Table of the Cattle Optimization Model

Number of Faces	Simplify efficiency	garland algorithm		New QEM algorithm	
		Maximum error	average error	Maximum error	average error
2400	44%	0.046337	0.082521	0.029240	0.007822
1300	20%	0.062643	0.016634	0.048874	0.017697
300	5%	0.330285	0.046763	0.162427	0.048233

As shown in Table 2, this time, the data test selected the prototype as the model of the car for optimization testing, and this test chose the number of different faces for comparison.

Table 2. Error Comparison Table of the Vehicle Optimization Model

Number of Faces	Optimization rate	garland algorithm		Optimize the QEM algorithm	
		Maximum error	average error	Maximum error	average error
7000	66%	0.028570	0.004493	0.025202	0.004824
4200	38%	0.053362	0.009993	0.040607	0.010858
1500	15%	0.113447	0.021826	0.064059	0.022998

Table 3. The Optimization Algorithm Saves Nodes and Schedules

	Original model		Simplified		Degree of savings%	
	Node(a)	Time(ms)	Node(a)	Time(ms)	Node	Time
Material A	8093	116	5630	75	69.5	64.4
Material B	202530	3249	162759	2912	81.3	90.0
Material C	9875	127	6541	98	65.2	64.1
Material D	12546	135	9875	115	71.2	70.2

According to Table 1 and Table 2, it can be seen that comparing the maximum error value, the maximum error value obtained by using the optimized QEM algorithm is much smaller than the maximum error value obtained by using the garland algorithm. According to the comparison of the average error value, it is found that the simplified model of the Garland algorithm is better than the optimized QEM algorithm, but the optimization is little. After using the optimized QEM

algorithm proposed in this article, the optimization of the model has a specific improvement compared to the Garland algorithm. As shown in Table 3, it saves about 50% of nodes in terms of nodes and nearly 90% of time and time under the premise of many optimizations.

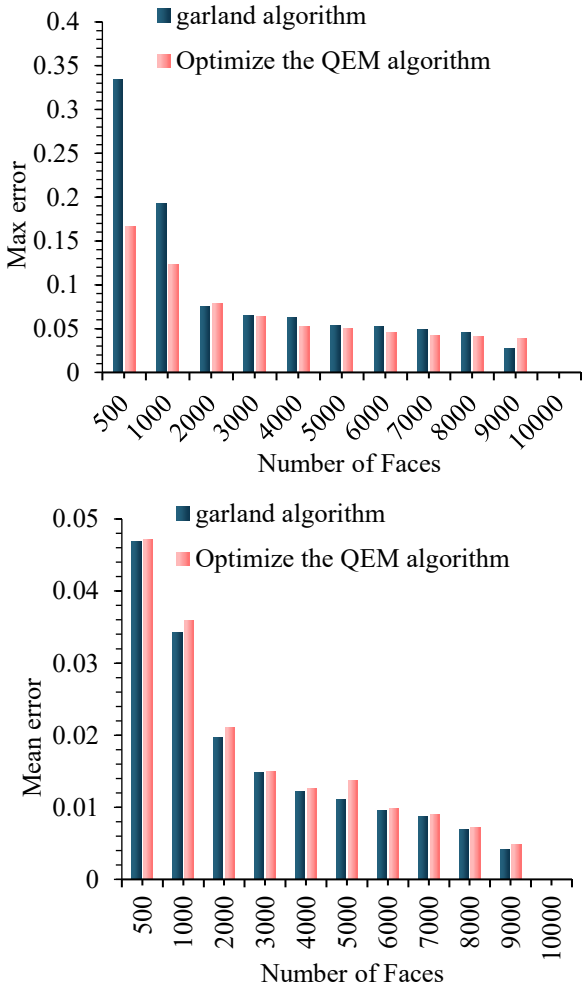

Fig.3 The maximum error and average error of the model at different resolutions

As shown in Figure 3, in the graph showing the maximum error value, the more significant error value of the garland algorithm is about 0.18 higher than the total value of the optimized QEM algorithm, and the average error value in the graph shows that the optimized QEM algorithm has a higher value than the garland algorithm.

3.2 Progressive Mesh Experiment of the Optimized Qem Algorithm

This experiment analyzes and verifies the specific performance of the algorithm with the time of constructing the progressive grid and the time of generating the detailed model of the advanced grid.

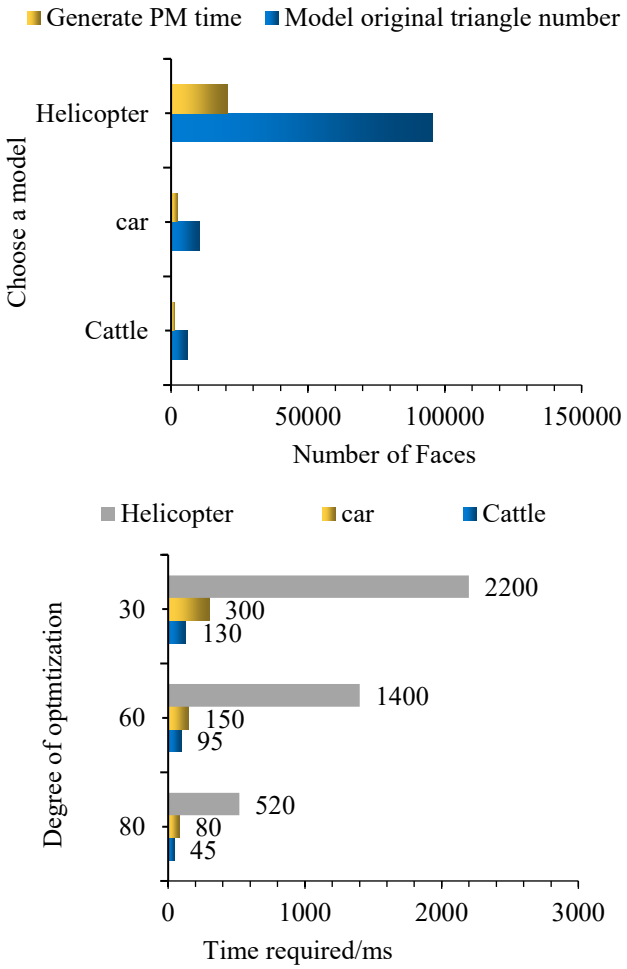

Fig.4 Model simplification and PM time chart

As shown in Figure 4, when the number of patches is less than 10,000, the time for PM generation is in the order of 10^1(s), which is entirely acceptable. In the optimization, when the original helicopter model is optimized to 30%, it takes 2200ms, and it takes 130ms to simplify the original model of the prototype to 30%.

3.3 Different Levels of Display Experiment of Progressive Grid Algorithm

This experiment compares the QEM algorithm with the optimized, simplified algorithm proposed in the article. It chooses an initial model with about 5900, then uses two algorithms to calculate, and finally analyzes the time to reduce to 10 faces according to the number of different looks.

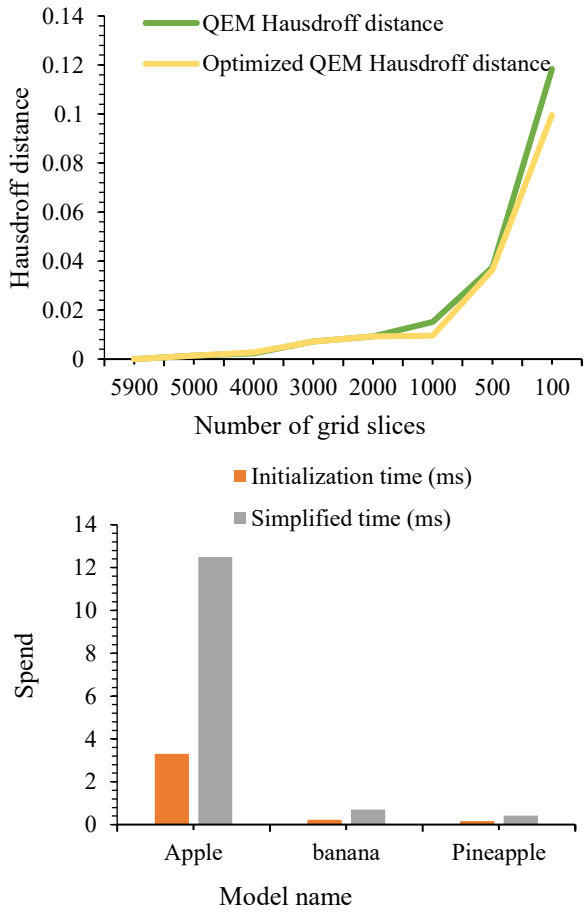

Fig.5 Grid realistic speed map

As shown in Figure 5, it takes about 12 seconds to simplify an initial model with nearly 70,000 faces to only ten faces, and each vertex of the model only needs a floating-point parameter, which shows that the algorithm can simplify complex models quickly.

3.4 Immune Genetic Algorithm Experiment

Two polyhedrons are selected, and their two different situations-collision and non-collision are tested separately. To facilitate the evaluation of the performance of the immune genetic algorithm, the experiment also simulates the general genetic algorithm and traditional collision detection, statistically compares the average results of the two algorithms, and draws experimental conclusions.

As shown in Figure 6, the immune genetic algorithm has a faster convergence rate than the other two algorithms regarding time complexity. It is also more accurate in terms of the accuracy of the shortest distance. When the population and the number of iterations change, there is no apparent fluctuation in the result.

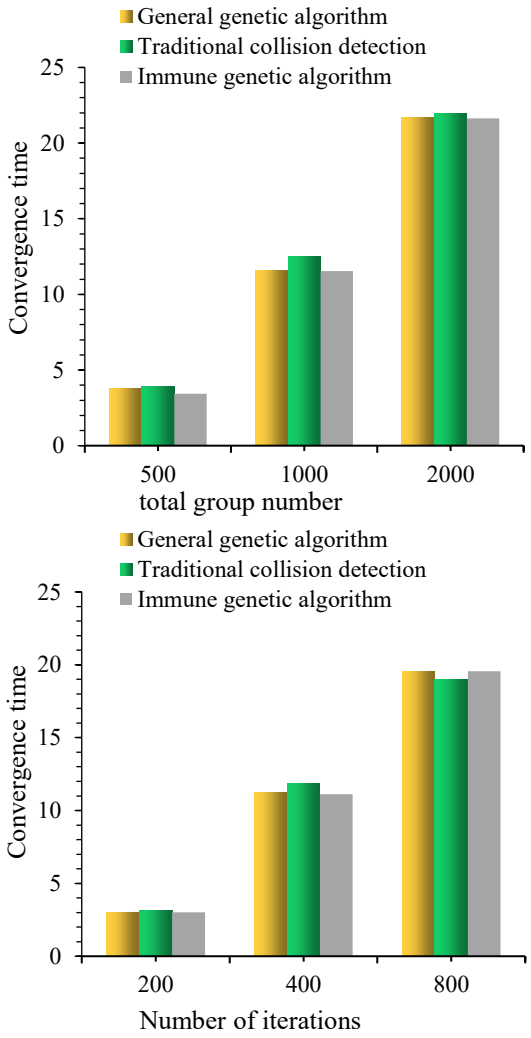

Fig.6 Data graph with different population numbers and iteration numbers

4 Discussion of Experimental Data

According to experiments, it is shown that the model can be simplified after the algorithm is simplified, and the simplification of the model simplifies not only the one-sided number of the model but also the generation time and the average distribution rate of the grid. Using the optimized QEM algorithm can make the grid distribution of the simplified model more even. When the population and the number of iterations change, there is no noticeable fluctuation in the result. From the algorithm's average convergence and affinity curves, we can also clearly know that the curve becomes smooth over time, converges to a particular value, the optimal solution is obtained, and the convergence speed is faster.

5 Conclusions

This article first explains the edge folding algorithm based on quadratic error. Because the error measurement proposed in this paper only considers the position information of the adjacent triangular grids, even after simplified processing, although the distribution of the grids will be more uniform, it will cause the sharp parts to lose features. Therefore, After the model is simplified accordingly, the absolute curvature of the vertex matrix is used as a new vertex error matrix. According to the experiments in this paper, the simplification based on the algorithm can still save the collection features of many original models, and the overall design of the model is also well maintained. Based on the improved progressive grid method, visual effects can be ensured, and grid models at all levels can be created quickly and efficiently.

Acknowledgment

Supported by Key Laboratory of Spatial Data Mining & Information Sharing of Ministry of Education, Fuzhou University (No.2023LSDMIS02).

Metacosmic Culture Laboratory, School of Journalism, Tsinghua University: Research on Simplification of LOD Grid Model in Virtual Reality Environment (No.H2022100162).

The Reform of Flight Training Mode Based on Educational Reform (No.XJ2022004501).

Conflicts of Interest

The authors declare no conflict of interest.

References

[1] Bell J T, Fogler H S. Preliminary testing of a virtual reality based educational module for safety and hazard evaluation training. 2022.

[2] Pestana-Santos M, Santos D, Jéssica Pinto, et al. Virtual Reality as a Nonpharmacological Strategy in Pediatric Pain Control During Procedures With Needle Use: An Integrative Review. Journal of Pediatric Surgical Nursing, 2021.

[3] Cui W, Na D E, Zhang Y. A Wireless Virtual Reality-Based Multimedia-Assisted Teaching System Framework under Mobile Edge Computing. Journal of Circuits, Systems and Computers, 2023, 32(07).

[4] Sharma A, Nett R, Ventura J. Unsupervised Learning of Depth and Ego-Motion from Cylindrical Panoramic Video with Applications for Virtual Reality. 2020.

[5] Amri A Y A, Osman M, Musawi A A. The Design Principles of 3D-Virtual Reality Learning Environment (3D-VRLE) in Science Education. 2021.

[6] Zhao C. Application of Virtual Reality and Artificial Intelligence Technology in Fitness Clubs. Mathematical Problems in Engineering, 2021, 2021(20):1-11.

[7] Hfab C, Hy A , Cc A. Large-scale terrain-adaptive LOD control based on GPU tessellation. Alexandria Engineering Journal, 2021, 60(3):2865-2874.

[8] Mai W, Fang L , Chen Z , et al. Application of the Somatosensory Interaction Technology Combined with Virtual Reality Technology on Upper Limbs Function in Cerebrovascular Disease Patients. Journal of Biomedical Science and Engineering, 2020, 13(5):66-73.

[9] Tatarinov V V, Kuzakov A S. Evaluation of the Characteristics of X-Ray Excitation under the Electron-Probe Effect Using 2D and 3D Modeling by the Monte Carlo Method. Journal of Surface Investigation: X-ray, Synchrotron and Neutron Techniques, 2020, 14(2):245-252.

[10] Wang X. Use network protocol to improve image and content search in mathematical calculation 3D modeling video analysis. AEJ - Alexandria Engineering Journal, 2021, 60(5):4473-4482.
[11] Valivand F, Katibeh H. Prediction of Nitrate Distribution Process in the Groundwater via 3D Modeling. Environmental Modeling & Assessment, 2020, 25(2):187-201.